


**ORIGINAL ARTICLE**

# Non-canonical IKB kinases regulate YAP/TAZ and pathological vascular remodeling behaviors in pulmonary artery smooth muscle cells

Aja Aravamudhan<sup>1</sup> | Paul B. Dieffenbach<sup>2</sup> | Kyoung Moo Choi<sup>1</sup> | Patrick A. Link<sup>1</sup> | Jeffrey A. Meridew<sup>1</sup> | Andrew J. Haak<sup>1</sup> | Laura E. Fredenburgh<sup>2</sup> | Daniel J. Tschumperlin<sup>1</sup> 

<sup>1</sup>Department of Physiology and Biomedical Engineering, Mayo Clinic, Rochester, Minnesota, USA

<sup>2</sup>Division of Pulmonary and Critical Care Medicine, Department of Medicine, Brigham and Women's Hospital, Boston, Massachusetts, USA

**Correspondence**

Daniel J. Tschumperlin, Department of Physiology and Biomedical Engineering, The Mayo Clinic, 200, First Street SW, Rochester, MN 55905, USA.

Email: [tschumperlin.daniel@mayo.edu](mailto:tschumperlin.daniel@mayo.edu)

**Funding information**

American Heart Association (AHA), Grant/Award Number: 20POST35210650 and 17GRNT33660449; Foundation for the National Institutes of Health (FNIH), Grant/Award Number: 5R01HL137366-04, K08 HL-143197, HL105355, HL158018 and HL153026

**Abstract**

Pulmonary arterial hypertension (PAH) causes pulmonary vascular remodeling, increasing pulmonary vascular resistance (PVR) and leading to right heart failure and death. Matrix stiffening early in the disease promotes remodeling in pulmonary artery smooth muscle cells (PASMCs), contributing to PAH pathogenesis. Our research identified YAP and TAZ as key drivers of the mechanobiological feedback loop in PASMCs, suggesting targeting them could mitigate remodeling. However, YAP/TAZ are ubiquitously expressed and carry out diverse functions, necessitating a cell-specific approach. Our previous work demonstrated that targeting non-canonical IKB kinase TBK1 reduced YAP/TAZ activation in human lung fibroblasts. Here, we investigate non-canonical IKB kinases TBK1 and IKK $\epsilon$  in pulmonary hypertension (PH) and their potential to modulate PASMCM pathogenic remodeling by regulating YAP/TAZ. We show that TBK1 and IKK $\epsilon$  are activated in PASMCs in a rat PH model. Inflammatory cytokines, elevated in PAH, activate these kinases in human PASMCs. Inhibiting TBK1/IKK $\epsilon$  expression/activity significantly reduces PAH-associated PASMCM remodeling, with longer-lasting effects on YAP/TAZ than treprostinil, an approved PAH therapy. These results show that non-canonical IKB kinases regulate YAP/TAZ in PASMCs and may offer a novel approach for reducing vascular remodeling in PAH.

**KEYWORDS**

non-canonical IKB kinases, pulmonary arterial hypertension, pulmonary artery smooth muscle cells, YAP and TAZ

**1 | INTRODUCTION**

Pulmonary arterial hypertension (PAH) is characterized by pulmonary vascular remodeling, increased pulmonary

vascular resistance (PVR), progressive pulmonary arterial (PA) stiffening (Malenfant et al., 2013), and ultimately right ventricular (RV) heart failure and death. Pulmonary artery smooth muscle cells (PASMCs) are one of the key cell types

This is an open access article under the terms of the [Creative Commons Attribution](https://creativecommons.org/licenses/by/4.0/) License, which permits use, distribution and reproduction in any medium, provided the original work is properly cited.

© 2024 The Authors. *Physiological Reports* published by Wiley Periodicals LLC on behalf of The Physiological Society and the American Physiological Society.

contributing to pathological vascular remodeling in PAH. While the biological mechanisms underlying PAH pathogenesis are incompletely understood, PA stiffening initiates a pathological feedback loop controlled by the mechanoregulatory transcription factors YAP/TAZ (Xie et al., 2018; Zuo et al., 2021). Pharmacological targeting of YAP/TAZ may thus provide a novel means to attenuate and/or reverse PAH and prevent RV dysfunction (Bertero et al., 2015; Pullamsetti et al., 2017). The prostacyclin pathway is one of the key targets of currently approved FDA treatments in PAH (Sitbon & Noordegraaf, 2017). Interestingly, recent work suggests that one of the mechanisms of action of prostacyclin analogs and prostacyclin receptor agonists may be via inhibition of YAP/TAZ (Dieffenbach et al., 2017; Zmajkovicova et al., 2019). However, due to the short half-life of prostacyclin, prostanoid therapy requires intravenous administration or frequent dosing, commonly leading to side effects, and may lead to complications such as catheter-related infections in patients requiring continuous infusion (Fares, 2015; Galie et al., 2009). These limitations of prostanoid therapy highlight the importance of developing new therapeutics that are both highly effective and long acting for the treatment of PAH.

TANK (TRAF-associated NF- $\kappa$ B activator) binding kinase 1 (TBK1) and IKK $\epsilon$  (also known as IKK-inducible or IKK-i) are termed the non-canonical IKB kinases (Peters et al., 2000; Pomerantz & Baltimore, 1999; Shimada et al., 1999). Prior studies have shown that TBK1/IKK $\epsilon$  can interact with YAP/TAZ leading to inhibition of TBK1/IKK $\epsilon$  activation during the host antiviral cellular response (Garcia et al., 2020; Zhang et al., 2017). We recently demonstrated that TBK1 can regulate TGF- $\beta$  signaling and the stability of transcription co-factors YAP/TAZ in human pulmonary fibroblasts (Aravamudhan et al., 2020), controlling their fibrogenic phenotype. Hence, the interaction between TBK1/IKK $\epsilon$  and YAP/TAZ is diverse and cell-type specific. In PAH, non-canonical IKB kinase pathway associated gene activation has been observed in genomic studies in pulmonary hypertension samples (Stearman et al., 2019) and in a meta-analysis of blood genome-wide expression profiling studies in PAH (Elinoff et al., 2020), suggesting potential relevance to PAH pathogenesis.

PAH progression is known to be driven by a multitude of interacting pathways. Mutation of the TGF- $\beta$  family member BMPRII has been observed in familial PAH (~27% of cases) (Aldred et al., 2006; Cogan et al., 2006; Newman et al., 2004), and dysregulation of BMPRII signaling has also been implicated in the pathogenesis of idiopathic PAH (Andruska & Spiekerkoetter, 2018). Numerous studies suggest that inflammation plays a key role in the development of pulmonary hypertension (PH) with strong evidence from animal models and human patient samples that exhibit inflammatory foci (Dorfmüller et al., 2003;

Rohm et al., 2019). Furthermore, inflammatory mediators that are known to activate non-canonical IKB kinases (Brasier, 2010; Patel et al., 2009; Yu et al., 2012) have been shown to be prognostic factors for worse outcomes in PAH (Dorfmüller et al., 2003). Further research has shown that the lack of protective effects from BMPRII signaling along with increased inflammatory activity (facilitated by cytokines like IL-6) may be a major factor promoting vascular remodeling of smooth muscle and endothelial cells of the pulmonary vasculature in PAH (Hagen et al., 2007; Hiepen et al., 2019; Steiner et al., 2009). The links between inflammatory and remodeling events in PAH remain to be fully elucidated.

We have shown previously that a mechanobiological feedback loop fueled by YAP/TAZ contributes to the sustained vascular remodeling pathology in PAH (Dieffenbach et al., 2017). While inflammatory cytokines such as IL-6 and transcriptional regulators YAP/TAZ play a pivotal role in PAH pathogenesis, they play several critical roles in cellular defense and regeneration and therefore cannot be directly targeted without undesirable effects. Studies on signaling by non-canonical IKB kinases have shown that their signaling is highly cell-type specific and dependent on the nature of the activating signal and the signaling subcomplex present in a given cell (Aravamudhan et al., 2020; Elinoff et al., 2020; Garcia et al., 2020; Stearman et al., 2019; Zhang et al., 2017). This renders the non-canonical IKB kinases as a complex signaling hub capable of differentially controlling several cellular processes and making them an attractive therapeutic target in diseases such as PAH. The continued discovery of chemical inhibitors of these kinases also offers a diverse toolkit to clinically modulate them (Aldred et al., 2006). Here, we tested if inhibition of TBK1/IKK $\epsilon$  would reduce YAP/TAZ activation and attenuate pathological vascular remodeling behaviors in human PSMCs.

## 2 | METHODS

### 2.1 | Animal models of PH

All animal experiments were performed in compliance with the relevant laws and guidelines as set forth by the Harvard Medical Area Standing Committee on Animals and the Lovelace Respiratory Research Institute Animal Care and Use Committee (IACUC) under IACUC-approved protocols. Adult male Sprague-Dawley rats (Charles River Laboratories) were injected with a single dose of monocrotaline (MCT) (50 mg/kg) or vehicle (PBS) subcutaneously (Landt et al., 2012). Animals were euthanized at 4 week, at which time lungs were snap-frozen in liquid nitrogen and stored at  $-80^{\circ}\text{C}$ . The primary

results from these animals were previously reported (Liu et al., 2016), including significant elevation in right ventricular systolic pressure, Fulton's index, and arterial wall thickness in response to MCT.

## 2.2 | Immunohistochemistry

The snap-frozen lungs were immersed in 20% sucrose solution, embedded in OCT, and sectioned as 10  $\mu$ m slices for histological staining, examination, and quantification. The rat lung tissue 10  $\mu$ m sections from control (vehicle treated) and MCT-treated rats were fixed in 4% PFA and stained for active (phosphorylated) TBK1 and IKK $\epsilon$  along with  $\alpha$ -SMA to mark the vascular smooth muscle cells in the pulmonary vasculature. The sections were blocked with 10% normal donkey serum/1% BSA/0.3M Glycine/0.5% Triton X100 in 1X TBS for 60 min. The sections were stained with primary antibody (Rabbit (DA1E) mAb IgG XP<sup>®</sup> Isotype Control, 1:100, 3900, Cell signaling technology; or rabbit anti-pTBK1(Ser172) 1:100, Bios-3400R, Bioss USA; or rabbit anti-pIKK $\epsilon$ (Ser172) 1:100, 06-1340, Millipore Sigma; along with goat anti- $\alpha$ -SMA 1:200, NB300-978, Novus biologics) diluted in antibody buffer (1% BSA, 0.5% Triton X100 in 1X TBS) and incubated at 4°C overnight, washed 3X with 1x TBST (0.25% Triton X100 in 1X TBS), followed by incubation with fluorescent dye conjugated secondary antibody (Alexa Fluor 555 Donkey anti-rabbit Ig-G 1:1000, A31572, Life Technologies; and Alexa Fluor 488 donkey anti-goat IgG 1:1000, A11055, Life Technologies) and DAPI (1:1000, 62248, Thermo scientific) in antibody buffer for 60 min at room temperature. Stained sections were washed 4x with 1x TBST, mounted in Aqua-Poly/Mount (Polyscience Inc., 18606) and cover slipped. The slides were dried overnight, sealed with clear nail polish, and imaged with a Keyence microscope at 20X, and 40X magnifications. The 40X images were used for quantification of active TBK1 and IKK $\epsilon$  in the smooth muscle cells of the pulmonary vasculature (identified by  $\alpha$ -SMA staining).

## 2.3 | Quantification of pTBK1 and pIKK $\epsilon$ staining in pulmonary vascular smooth muscle cells

Immunofluorescent staining of pTBK1 and pIKK $\epsilon$  were analyzed in the  $\alpha$ -SMA positive pulmonary vascular wall cells. Thresholding followed by pixel intensity and area quantification were performed using ImageJ. The pixel intensity of the stain was normalized to the section's area. All quantification was performed on 10 or more randomly chosen images per sample (Aravamudhan et al., 2018;

Ruffenach et al., 2019).  $N=4$  samples/group were used for control and MCT samples.

## 2.4 | Cell culture

Primary Pulmonary Artery Smooth Muscle Cells (PASMCs) (Human PASMCs, lot no. 0000669096 and lot no. 0000701036) were purchased from Lonza (Walkersville, MD). 0000669096 and 0000701036 were derived from 51-year-old and 58-year-old Male Caucasian patients, respectively. Control and PAH PASMCs were derived from explanted lungs of patients with group 1 PAH who underwent lung transplantation or from control donor lungs not suitable for transplantation as part of the Pulmonary Hypertension Breakthrough Initiative (PHBI) under a protocol approved by the Partners Human Research Committee. Informed consent was obtained by the PHBI subjects or their legal guardians before they enrolled in the study. Primary idiopathic pulmonary arterial hypertension (IPAH) PASMCs and control PASMCs were studied as in prior work (Dieffenbach et al., 2017). IPAH Donor 1 and matched Control Donor 1 PASMCs were from 32- and 36-year-old female subjects, respectively. IPAH Donor 2 and matched control Donor 2 PASMCs were from 25-year-old male patients, respectively. Cell lines tested negative for human immunodeficiency virus, hepatitis B, hepatitis C, mycoplasma, bacteria, yeast, and fungi. PASMCs were cultured in smooth muscle basal medium (SmBM) supplemented with 5% FBS, SmGM-2 SingleQuots (Lonza), penicillin (100 IU/m), and streptomycin (100  $\mu$ g/mL) in a humidified incubator (21% O<sub>2</sub>, 5% CO<sub>2</sub>) at 37°C. All primary cell culture experiments were performed with cells at passage six or less.

## 2.5 | Chemical inhibitors

The following chemical inhibitors were used: treprostinil (Compound CID: 91617675) a potent prostacyclin (PGI<sub>2</sub>) analog (Tocris), inhibitors of TBK1/IKK $\epsilon$ : Amlexanox (Compound CID:2161)(Tocris), TBK1/IKK $\epsilon$ -IN-1(compound I) (CI) (Compound CID: 124156234) (Selleckchem), and TBK1/IKK $\epsilon$ -IN-2 (compound II) (CII) (Selleckchem). The chemical stocks were prepared using DMSO as the solvent and all the experiments used DMSO as a control.

## 2.6 | Cytokine treatment

PASMCs were seeded at a density of 25 cell/mm<sup>2</sup> in 24-well plates and cultured at 37°C and 5% CO<sub>2</sub>. DMEM/

F12 media was used with 5% FBS. Following cellular attachment, the cells were serum starved (SS) in DMEM/F12 with 0.5% FBS, penicillin (100 IU/ml), and streptomycin (100 µg/ml) overnight. PSMCs were subsequently treated with SS media, high serum (HS) media (DMEM/F12 and 20.0% FBS, penicillin (100 IU/ml), and streptomycin (100 µg/ml)), TNF- $\alpha$  (20 ng/ml), IL-1 $\beta$  (10 ng/ml), or ET-1 (100 ng/ml). DMEM/F12 and HS (20.0% FBS, penicillin (100 IU/ml), and streptomycin (100 µg/ml)) media was used as the positive control. The cells were lysed, and the contents collected after 2 h of treatment. For YAP/TAZ staining, the same protocol was followed while the cells were seeded in a 96 well plate and fixed after 2 h for immunostaining.

## 2.7 | TBK1/IKK $\epsilon$ plasmid transfection

pcDNA3-Flag-TBK1 and pcDNA3-Flag-TBK1(K38A) were generously donated by Dr. Fitzgerald (UMass Medical, Boston) (Fitzgerald et al., 2003). pcDNA3 IKK $\epsilon$  Flag, pcDNA3 IKK $\epsilon$  K38A Flag (Fitzgerald et al., 2003), and Flag pcDNA3 (Sanjabi et al., 2005) were purchased from Addgene. Briefly, the plasmids were transformed into competent cells after recovery, as per the manufacturer's instructions. LB agar plates with appropriate antibiotics were used to select the colonies by incubating at 37°C overnight. These selected colonies expressing the plasmids of interest were further scaled up and cultured in sterile LB broth with Carbenicillin. After incubation for 18 h, the culture was spun down in a centrifuge to isolate the bacterial plasmids. Plasmids were purified using a Maxiprep kit (Qiagen). The purified plasmids were dissolved in TE buffer and spectrophotometrically quantified. PSMCs were seeded in 6-well plates and allowed to reach 80% confluence. Lipofectamine 3000 reagent (Thermo Fisher Scientific) was used to transfect 2.5 µg of plasmid per reaction.

## 2.8 | Western blot analysis

PASMCs were plated in six-well plates. For studies measuring phosphorylated and total TBK1/IKK $\epsilon$  in cells treated with cytokines/chemicals, the cells were plated, and serum starved overnight, and then, media with cytokine/chemicals was added to the media for 2 h before protein isolation and blotting for TBK1/IKK $\epsilon$  activation. A seeding density of 50 cells/mm<sup>2</sup> was used in all experiments. In all experiments, the total protein was isolated using RIPA buffer (pH 8.0) with Pierce Phosphatase Inhibitor (Thermo) and Halt Protease Inhibitor Cocktail (Thermo). Total protein

concentration of the lysates was determined using a Pierce BCA Protein Assay Kit (Thermo), and samples were run on a 7.5% polyacrylamide gel. Proteins were then transferred from the gel to a nitrocellulose membrane. The following primary antibodies were used for overnight incubation of these blots: anti-phospho-TBK1/NAK (Ser172) (D52C2) XP Rabbit mAb (5483 T; Cell Signaling Technology), Anti-phospho-IKK-epsilon (Ser172) (06-1304; Millipore-Sigma), Anti-NAK/TBK1 antibody (EP611Y) (ab40676; Abcam, Cambridge, MA), Anti-IKK $\epsilon$  (D20G4) Rabbit mAb (2905S; Cell Signaling Technology), Anti-YAP/TAZ rabbit mAb (8418S; Cell Signaling Technology), and GAPDH (14C10; Cell Signaling Technology). All antibodies were diluted in 5% BSA/TBST. Phospho-TBK1 was diluted at 1:250, and phospho-IKK $\epsilon$  and IKK $\epsilon$  were diluted at 1:500 and TBK1 at 1:1000. Blots were washed with TBS-Tween before 60 min incubation with anti-rabbit-HRP-conjugated secondary (W4011; Promega) antibody diluted 1:3000 in 5% BSA/TBST. Membranes were imaged using a Bio-Rad ChemiDoc Imaging system (Hercules, CA) with quantification performed via densitometry using NIH-Fiji software. Each antibody produced one obvious band of the appropriate size, and TBK1 and IKK $\epsilon$  antibodies were validated using TBK1 and IKK $\epsilon$  siRNA.

## 2.9 | Immunostaining

PASMCs were plated in clear-bottom 96-well plates at a density of 50 cells/mm<sup>2</sup> in DMEM/F12 (Gibco) containing SS media overnight as described above. In experiments testing CII, the different concentrations of the drug were diluted in cell culture media before cell treatment. In siRNA experiments, PSMCs were first transfected with control or (TBK1+IKK $\epsilon$ )-siRNA for 24 h, reseeded on a 96-well plate, SS media for 48 h. Cells were fixed in 3.7% formalin (Sigma), permeabilized with 0.25% Triton X-100 (Sigma-Aldrich), and then blocked with 5% BSA for 1 h. Cells were incubated overnight with a FITC-conjugated mouse monoclonal antibody against YAP/TAZ (D24E4; Cell Signaling Technology) diluted 1:200 in PBS with 1% BSA. Finally, the cells were counterstained with DAPI nuclear stain. Cells were then washed and imaged using a Cytation 5 imaging system (Bio-Tek) at 10 X magnification. YAP/TAZ localization was quantified using Gen5 (Biotek) software. For this purpose, cell nuclei were identified using the DAPI channel and YAP/TAZ nuclear staining intensity was first quantified in sparsely seeded PSMCs as a positive control. A threshold value of 90% of this intensity was then set to quantify the cells positive for nuclear YAP/TAZ. The percentage of YAP/TAZ nuclear positive cells after treatments was thus calculated (Haak et al., 2019).

## 2.10 | SiRNA transfection

Control, IPAH subject, and Lonza PSMCs were transfected using Lipofectamine RNAiMAX (Life Technologies) with an siRNA (Dharmacon, Lafayette, CO) containing four siGENOME Human TBK1 (29110) and siGENOME Human IKBKE (9641) siRNA or a nontargeting SMARTpool control. Cells were seeded at a density of 100 cells/mm<sup>2</sup> in 24-well plates using SS media, as described above, and treated with 10 nM of each targeting siRNA SMARTpool or equivalent amounts of nontargeting siRNA for at least 16 h, with a reference sample collected at the time of siRNA treatment to serve as a baseline control. Knockdown of each siRNA target was confirmed by RT-PCR and western blotting 72 h after transfection. Gene expression analysis was performed by qPCR to confirm knockdown. Cells received different treatments as indicated in each experiment. RNA was isolated using the RNeasy Plus Mini Kit (Qiagen, Germantown, MD) as per the manufacturer's protocol. Isolated RNA was used to synthesize cDNA using SuperScript VILO (Invitrogen Life Technologies). Fast Start Essential DNA Green Master (Roche) was used to perform quantitative PCR analysis using a LightCycler 96 (Roche) machine.  $\Delta\Delta C_t$  calculation was used relative to 16srRNA (16s) to determine the fold change in gene expression of the samples with respect to the nontreated controls.

## 2.11 | Cell proliferation

Proliferation was assessed using the BrdU Cell Proliferation colorimetric ELISA Kit (Abcam, Boston, MA) as per the manufacturer's protocol. PSMCs were seeded using a sterile 96-well tissue culture plate at a density of  $2 \times 10^5$  cells/mL in 100  $\mu$ L/well of appropriate cell culture media. Some of the wells on the plate were used for controls: wells that do not contain cells (media alone) and wells which contain cells but did not receive the BrdU reagent (assay background). In total, 20  $\mu$ L of the diluted 1X BrdU reagent was added to each well 24 h before harvest for every timepoint. At set timepoints, the plates were harvested by adding 200  $\mu$ L/well of the fixing solution and incubated at room temperature for 30 min to fix the cells and denature the DNA to be assayed for BrdU incorporation. The plates were washed and incubated with 100  $\mu$ L/well of anti-BrdU monoclonal Detector Antibody for 1 h at room temperature. The plates were washed and incubated with 100  $\mu$ L/well of 1X Peroxidase Goat Anti-Mouse IgG Conjugate for 30 min. Plates were washed with distilled water and dried off by patting, and 100  $\mu$ L/well of TMB Peroxidase

substrate was added and incubated for 30 min at room temperature in the dark. The plates were read on a spectrophotometric plate reader at 450/550 nm. A standard curve with known numbers of cells was used to calculate the proliferation percentages.

## 2.12 | Cell viability and apoptosis

Cellular viability and apoptosis were measured using an Apo-Glo<sup>®</sup> Live multiplex assay (Promega, Madison, WI) as per the manufacturer's protocol. Briefly, the cells were plated as above on a white assay plate specifically used for the Apo-Glo Live assay. At the end of each timepoint, 10  $\mu$ L of substrate was transferred into 2 mL of Assay Buffer. In total, 20  $\mu$ L of viability reagent was added to all wells, and briefly mixed by orbital shaking (300–500 rpm for ~30 s). The cells were incubated for 30 min at 37°C. Fluorescence was measured at the following wavelength: 400Ex/505Em. Fluorescence was used as directly proportional to cell viability (RFU).

Apoptosis: Caspase-Glo<sup>®</sup> 3/7 Buffer and lyophilized Caspase-Glo<sup>®</sup> 3/7 Substrate were equilibrated to room temperature before use. The contents of the Caspase-Glo<sup>®</sup> 3/7 Buffer bottle were transferred into the amber bottle containing the Caspase-Glo<sup>®</sup> 3/7 Substrate. The contents were mixed until the substrate was thoroughly dissolved to form the Caspase-Glo<sup>®</sup> 3/7 Reagent. In total, 100  $\mu$ L of Caspase-Glo<sup>®</sup> 3/7 Reagent was added to each sample in the 96-well plate containing 100  $\mu$ L of media. Samples were mixed gently using a plate shaker and incubated at room temperature for 30 min. The luminescence of the samples was measured in a plate-reading luminometer as caspase (apoptotic) activity and normalized to cellular viability.

## 2.13 | Cell numbers

PASMC cell number was quantified using a CyQUANT<sup>®</sup> assay (Thermo Fisher scientific Waltham, MA) as per the manufacturer's protocol. Briefly, PSMCs were seeded in 96-well plates as above. The microplates were emptied by gentle inversion and blotted onto paper towels to remove medium from the wells. The wells were washed carefully with phosphate buffered saline (PBS), frozen and stored at  $-70^\circ\text{C}$  until samples were assayed. The concentrated cell-lysis buffer stock solution (Component B) was diluted 20-fold in distilled water. The CyQUANT<sup>®</sup> GR stock solution (Component A) was diluted 400-fold in the 1X cell-lysis buffer. The plates were thawed at room temperature. Then, 200  $\mu$ L of the CyQUANT<sup>®</sup> GR dye/cell-lysis buffer

was added to each sample well. It was mixed gently and incubated for 2–5 min at room temperature, protected from light. The sample fluorescence was measured using a fluorescence microplate reader with filters appropriate for ~480 nm excitation and ~520 nm emission maxima. A standard curve was used to determine the cell number from the fluorescence values obtained in the assay.

## 2.14 | Gene expression analysis by qPCR

Cells received different treatments as indicated in each experiment before RNA isolation using the RNeasy Plus Mini Kit (Qiagen) as per the manufacturer's protocol. Isolated RNA was used to synthesize cDNA using SuperScript VILO (Invitrogen Life Technologies). Fast Start Essential DNA Green Master (Roche) was used to perform quantitative PCR analysis using a LightCycler 96 (Roche) machine.  $\Delta\Delta C_t$  calculation was used relative to 16srRNA (16s) to determine the fold change in gene expression of the samples with respect to the nontreated controls.

<b>Human-YAP1-F</b>	<b>TGTCCCAGATGAACGTCACAGC</b>
Human-YAP1-R	TGGTGGCTGTTTCACTGGAGCA
<b>Human-WWTR1-F</b>	<b>GAGGACTTCCTCAGCAATGTGG</b>
Human-WWTR1-R	CGTTTGTTCTGGAAGACAGTCA
<b>Human-CTGF-F</b>	<b>GTCCAGCACGAGGCTCA</b>
Human-CTGF-R	TCGCCTTCGTGGTCCTC
<b>Human-CYR61-F</b>	<b>CTCGCCTTAGTCGTACCC</b>
Human-CYR61-R	CGCCGAAGTTGCATTCCAG
<b>Human-TBK1-F</b>	<b>TGCACCCTGATATGTATGAGAGA</b>
Human-TBK1-R	AAATGGCAGTGATCCAGTAGC
<b>Human-IKBKE-F</b>	<b>GAGAAGTTCGTCTCGGTCTATGG</b>
Human-IKBKE-R	TGCATGGTACAAGGTCACCTCC
<b>Human-16srRNA-F</b>	<b>GCTTTCCTTTTCCGGTTGCG</b>
Human-16srRNA-R	ACACGGATGTCTACACCAGC

## 2.15 | Traction force microscopy

As previously described (Marinković et al., 2012), polyacrylamide gel substrates with 13 kPa Young's moduli were prepared, and fluorescent sulfate-modified latex microspheres (0.2  $\mu$ m, 505/515 excitation/emission, FluoSpheres; Life Technologies) were conjugated to the gel surfaces after treatment with 1 mg/mL of dopamine hydrochloride (Sigma-Aldrich) in 50 mM HEPES solution (pH 8.5) for 20 min, followed by treatment with type 1 collagen solution (Advanced Biomatrix). Cells were plated on the gels and switched to DMEM/F12 containing 2% FBS overnight. For inhibitor experiments, the drug was

added to the culture media with TGF- $\beta$  (6 ng/mL) and ET-1 (100 ng/mL). In siRNA experiments, PSMCs were first transfected with control or TBK1/IKBKE siRNA and then reseeded on gels after a 24-h transfection period. Images of gel surface-conjugated fluorescent beads were obtained for cells before and after trypsinization using a Cytation5 imaging system (Bio-Tek) at 10X magnification. TractionForAll (<https://www.mayo.edu/research/labs/tissue-repair-mechanobiology/software>) software was used to measure the two-dimensional traction forces by measuring bead displacement fields and computing corresponding traction fields.

## 2.16 | Statistical analysis

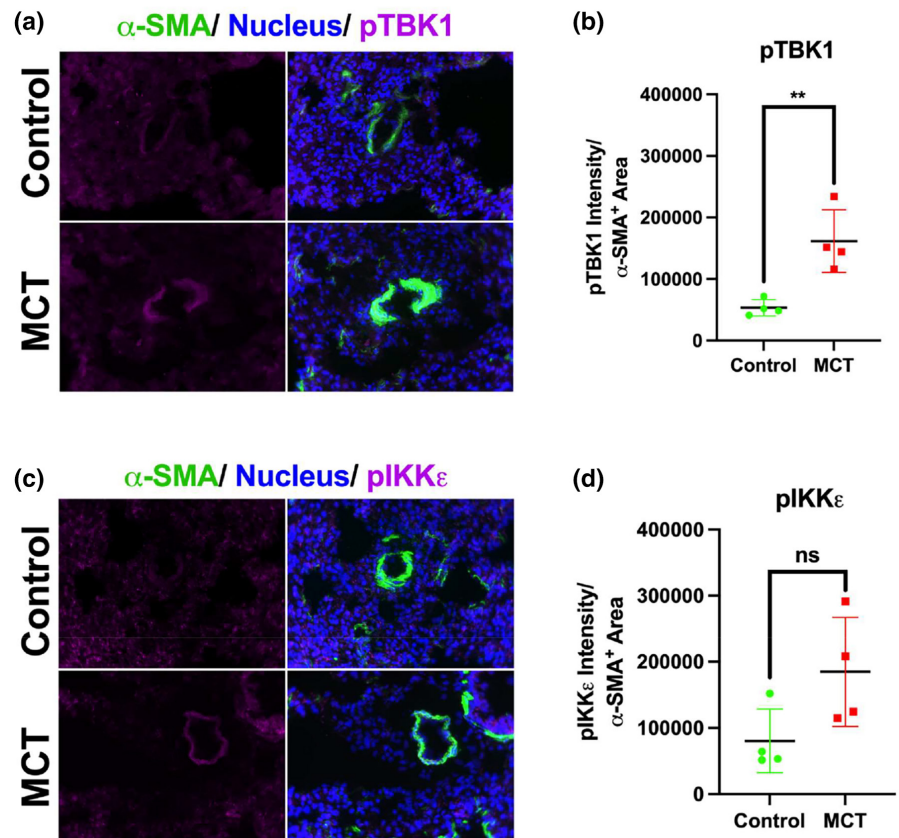
Data are shown as means  $\pm$  SD. Comparisons involving multiple groups were performed using one-way ANOVA with Tukey post-test. Comparisons involving subgroups were performed using a two-way ANOVA with a multiple-comparison post-test. Comparisons involving two groups were performed using a t-test (GraphPad Prism v 8.0; GraphPad Software, San Diego, CA).  $p < 0.05$  was considered significant.

## 3 | RESULTS

### 3.1 | TBK1/IKK $\epsilon$ are activated in the pulmonary vasculature of MCT-induced PH in rats

To examine if non-canonical IKB kinases are activated in PSMCs in experimental PH, lungs from a previously published study (Liu et al., 2016) of monocrotaline (MCT)-induced PH rats were histologically analyzed. Vehicle control and MCT-treated rat lungs were stained using antibodies against activated TBK1 and IKK $\epsilon$ , with  $\alpha$ SMA co-staining used to identify smooth muscle cells in the pulmonary vascular wall (green). Active TBK1 and IKK $\epsilon$  were stained with pTBK1 (purple) (Figure 1a) and pIKK $\epsilon$  antibodies (purple) (Figure 1c). The intensity of the signals in the  $\alpha$ SMA-expressing pulmonary vascular smooth muscle cells was quantified and normalized to the vessel wall area. Expression of active pTBK1 was significantly higher in MCT-treated rats compared with vehicle-treated controls (Figure 1b). There was a trend toward increased expression of pIKK $\epsilon$  in MCT rats compared to controls (Figure 1d,  $p = 0.07$ ), but expression was highly variable among animals. These results are consistent with increased activation of non-canonical IKB kinases TBK1 and IKK $\epsilon$  in PSMCs in experimental PH.

**FIGURE 1** Activation of TBK1/IKK $\epsilon$  in pulmonary vasculature of MCT rats. Histological sections from the lungs of Control (vehicle) treated vs monocrotaline (MCT) treated rats after 4 weeks of treatment were stained for (a) active pTBK1 (purple)/nucleus (DAPI) (blue) and smooth muscle cells ( $\alpha$ -SMA) (green) and (c) active pIKK $\epsilon$  (purple)/nucleus (DAPI) (blue) and smooth muscle cells ( $\alpha$ -SMA) (green). A minimum of 10 vessels were captured per rat, and the pTBK1 (b) and pIKK $\epsilon$  (d) protein fluorescent intensity within the smooth muscle ( $\alpha$ -SMA+ area) was measured for each vessel and averaged. Groups were compared by unpaired *t*-test with \*\* indicates *p* value <0.01. Data represent four biological samples per condition. Scalebar represents 100  $\mu$ m.



### 3.2 | Cytokine stimulation of PSMCs increased TBK1/IKK $\epsilon$ and YAP/TAZ activation

Serum levels of cytokines such as TNF- $\alpha$  and IL-1 $\beta$  are increased in the serum of patients with PAH, and higher serum inflammatory cytokines are associated with poor survival in PAH over time (Cracowski et al., 2014; Soon et al., 2010). TNF- $\alpha$  overexpression has been shown to increase lung volumes and induce PH in mice (Fujita et al., 2001; Stevens et al., 1992). TNF- $\alpha$  treatment suppresses prostacyclin expression in rat PSMC (Itoh et al., 2003) and increases pulmonary vascular reactivity in isolated rat lungs (Stevens et al., 1992). Additionally, inhibition of TNF- $\alpha$  and IL-1 $\beta$  have been shown to attenuate MCT-induced PH in rats (Voelkel et al., 1994; Wang et al., 2013). Endothelin-1 (ET-1) is a mediator of vasoconstriction in PAH and can also induce hyperproliferation of cells of the pulmonary vasculature, a hallmark of PAH. Given increased activation of non-canonical IKB kinases in the MCT model of PH, we next assessed the effects of cytokine stimulation on activation of non-canonical IKB kinases in PSMCs. Human PSMCs were stimulated with TNF- $\alpha$ , IL-1 $\beta$ , or ET-1 and activation of TBK1 and IKK $\epsilon$  (phosphorylated levels relative to total levels) were assessed at serial time points over 2 h. TNF- $\alpha$  significantly increased TBK1 activation (Figure 2a),

while IL-1 $\beta$  significantly increased activation of IKK $\epsilon$  (Figure 2b). TBK1 had a modest response to ET-1 that failed to reach statistical significance (Figure 2c). Given the role of YAP/TAZ in PSMC activation (Dieffenbach et al., 2017) and given that TBK1 regulates YAP/TAZ activation in lung fibroblasts (Aravamudhan et al., 2020), we next examined the effect of these cytokines on YAP/TAZ activity in PSMCs. Treatment with TNF- $\alpha$ , IL-1 $\beta$ , and ET-1 all increased nuclear (active) YAP/TAZ expression (Figure 2d) in serum-starved PSMCs, similar to the high serum (HS) positive control. These results show that cytokines implicated in PAH activate non-canonical IKB kinases and YAP/TAZ in human PSMCs.

### 3.3 | Reducing TBK1/IKK $\epsilon$ levels/activity in PSMCs decreases YAP/TAZ activation

To examine if biological silencing and chemical inhibition of TBK1/IKK $\epsilon$  reduces activation of YAP/TAZ in PSMCs, siRNA, plasmid vector, and chemical inhibitors targeting TBK1/IKK $\epsilon$  were administered to PSMCs (Figure 3). SiRNA against control (si-Scr), TBK1 (si-TBK1), IKK $\epsilon$  (si-IKK $\epsilon$ ), and a combination of TBK1/IKK $\epsilon$  (si-TBK1+IKK $\epsilon$ ) were administered to PSMCs. Nuclear YAP/TAZ levels were determined by imaging after immunostaining (Figure 3a), and the relative nuclear YAP/TAZ was

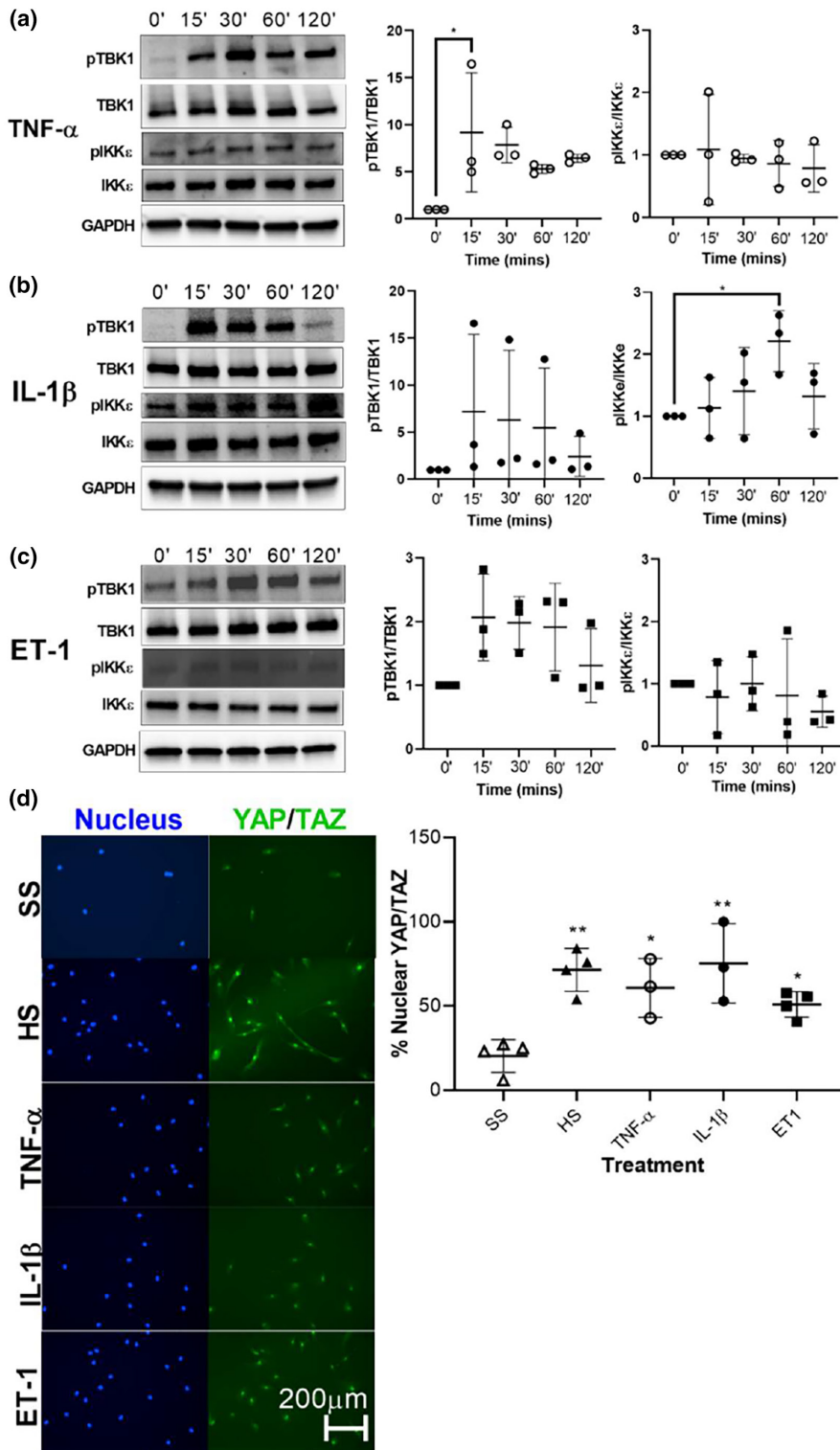


**FIGURE 2** Effect of cytokine stimulation on PASM TBK1/IKK $\epsilon$  activation. PASM cells were stimulated with cytokines associated with PAH including (a) TNF- $\alpha$  (20 ng/mL), (b) IL-1 $\beta$  (10 ng/mL), or (c) ET-1 (100 ng/mL). Total and phosphorylated TBK1, IKK $\epsilon$ , and total GAPDH were quantified by densitometry. (d) PASM cells were serum starved or stimulated with high serum-HS (20.0% FBS) media or cytokines TNF- $\alpha$ , IL-1 $\beta$ , or ET-1 as above. Nuclear (active) YAP/TAZ in PASM cells was quantified by counting immunopositive. One-way ANOVA with Tukey post-test was used for both analyses, with significance designated \*  $p < 0.05$ , \*\*  $p < 0.01$ . Horizontal lines indicate mean values. Data represent 3–4 biological experiments. Scalebar represents 200  $\mu$ m.

quantified (Figure 3b). Combined knockdown of TBK1/IKK $\epsilon$  (si-TBK1+IKK $\epsilon$ ), but not individual knockdown, significantly decreased YAP/TAZ nuclear levels in PASM cells. To examine the effect of reducing TBK1 and IKK $\epsilon$  on total protein levels of YAP/TAZ, PASM cells were treated with scramble control (si-Scr), TBK1 (si-TBK1), IKK $\epsilon$  (si-IKK $\epsilon$ ), and a combination of TBK1/IKK $\epsilon$  (si-TBK1+IKK $\epsilon$ ). Total protein was extracted and examined by western blot analysis

(Figure 3c). Total protein levels of YAP and TAZ were significantly reduced in the si-TBK1+IKK $\epsilon$  group compared with si-Scr control cells (Figure 3d). Like the effects on YAP/TAZ nuclear levels, individual silencing of TBK1 or IKK $\epsilon$  alone did not significantly impact YAP or TAZ expression in PASM cells. These results show that silencing non-canonical I $\kappa$ B kinase expression significantly reduces total and active (nuclear) YAP/TAZ levels in human PASM cells.



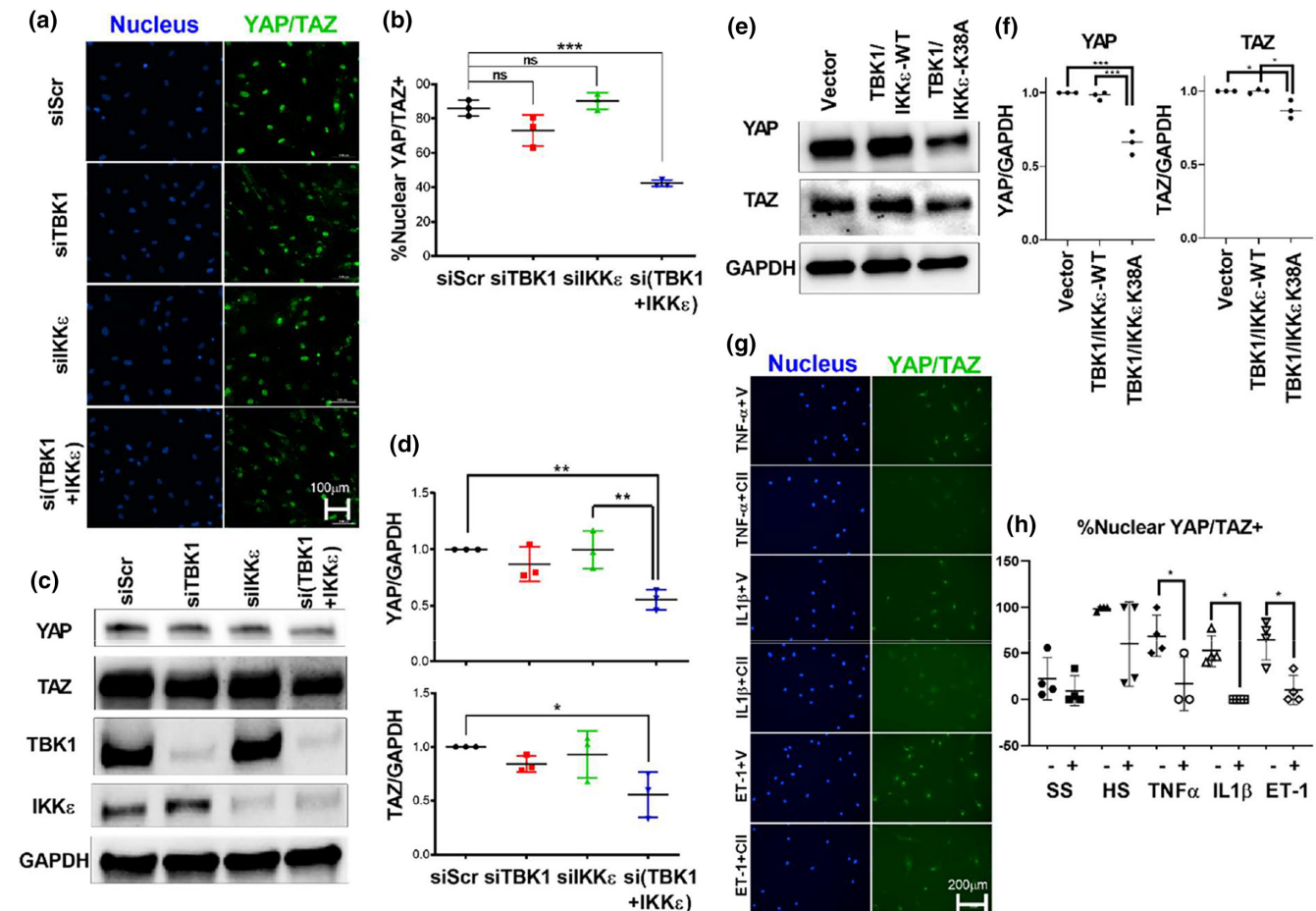


**FIGURE 3** Reducing TBK1/IKK $\epsilon$  decreases YAP/TAZ activation. (a) and (b): siRNA against TBK1 or IKK $\epsilon$  alone did not reduce nuclear YAP/TAZ, but combined siRNA against both TBK1 and IKK $\epsilon$  reduced nuclear YAP/TAZ significantly in PASCs. (c) and (d) reducing TBK1 and IKK $\epsilon$  on PASCs together, significantly reduced the total protein levels of YAP/TAZ. (e) and (f): PASCs transfected with kinase deficient TBK1K38A and IKK $\epsilon$ K38A mutants had significantly lower levels of YAP and TAZ than wildtype (WT) and empty vector transfected cells. (g) and (h) Cytokine stimulation nuclear YAP/TAZ in PASCs with TNF- $\alpha$ , IL-1 $\beta$ , and ET-1 was reduced to baseline with a small molecule inhibitor (Compound II, +) compared to vehicle control (V, -) in each of the treatments. One-way ANOVA with Tukey post-test: Significance designated \* $p < 0.05$ , \*\* $p < 0.01$ , and \*\*\* $p < 0.001$ . Horizontal lines indicate mean values. Data represent three or more biological experiments. Scalebar represents 100 or 200  $\mu\text{m}$  as indicated.

To determine if directly targeting the activity of non-canonical I $\kappa$ B kinases affects YAP/TAZ expression, a plasmid containing vector control (Vector), wild type TBK1 and IKK $\epsilon$  (TBK1/IKK $\epsilon$ -WT), and kinase dead mutants TBK1K38A and IKK $\epsilon$ K38A (TBK1/IKK $\epsilon$ -K38A) were transfected into PASCs. Western blot was run for YAP and TAZ (Figure 3e). Cells transfected with kinase dead mutants TBK1/IKK $\epsilon$ -K38A showed significantly decreased expression of YAP and TAZ compared with TBK1/IKK $\epsilon$ -WT-transfected and control (vector) PASCs (Figure 3f). These results suggest that the catalytic activity of TBK1/IKK $\epsilon$  may be necessary to actively maintain protein levels of YAP/TAZ in PASCs.

To further assess the effect of targeting non-canonical I $\kappa$ B kinases chemically on YAP/TAZ nuclear localization, we treated cytokine-stimulated PASCs with the non-canonical I $\kappa$ B kinase inhibitor Compound II (+)

compared with vehicle (-) (Figure 3g). Cells were imaged after immunostaining for nuclear YAP/TAZ which demonstrated that CII treatment reversed cytokine-stimulated activation of YAP/TAZ in PASCs (Figure 3h). This further suggests that reducing the catalytic activity of non-canonical I $\kappa$ B kinases attenuates YAP/TAZ activation in PASCs.

### 3.4 | TBK1/IKK $\epsilon$ knockdown attenuates pathological vascular remodeling behaviors and YAP/TAZ function in PAH-PASC

Pathologic hallmarks of PASCs in PAH include excessive proliferation and resistance to apoptosis leading to an increase in cell number. We have also demonstrated

enhanced contractility, assessed by traction force microscopy, in PAH PASC (Dieffenbach et al., 2017). Our prior work showed that YAP/TAZ activity is increased in PAH PASC and necessary for stiffness-induced remodeling phenotypes. To establish the relationship between non-canonical IKK kinases and PASC pathological phenotype development, we knocked down TBK1/IKK $\epsilon$  in PASCs using siRNA (siTBK1+IKK $\epsilon$ )

and compared the effects to knockdown of a scramble control (siScr). PASCs were then stimulated to proliferate in 20% FBS-containing media, and a control group was maintained with 2% FBS-containing media. Control samples were harvested and analyzed at the time of siRNA treatment to serve as a baseline. We assessed the effects of TBK1/IKK $\epsilon$  knockdown on PASC total cell number (Figure 4a), proliferation (by BrdU

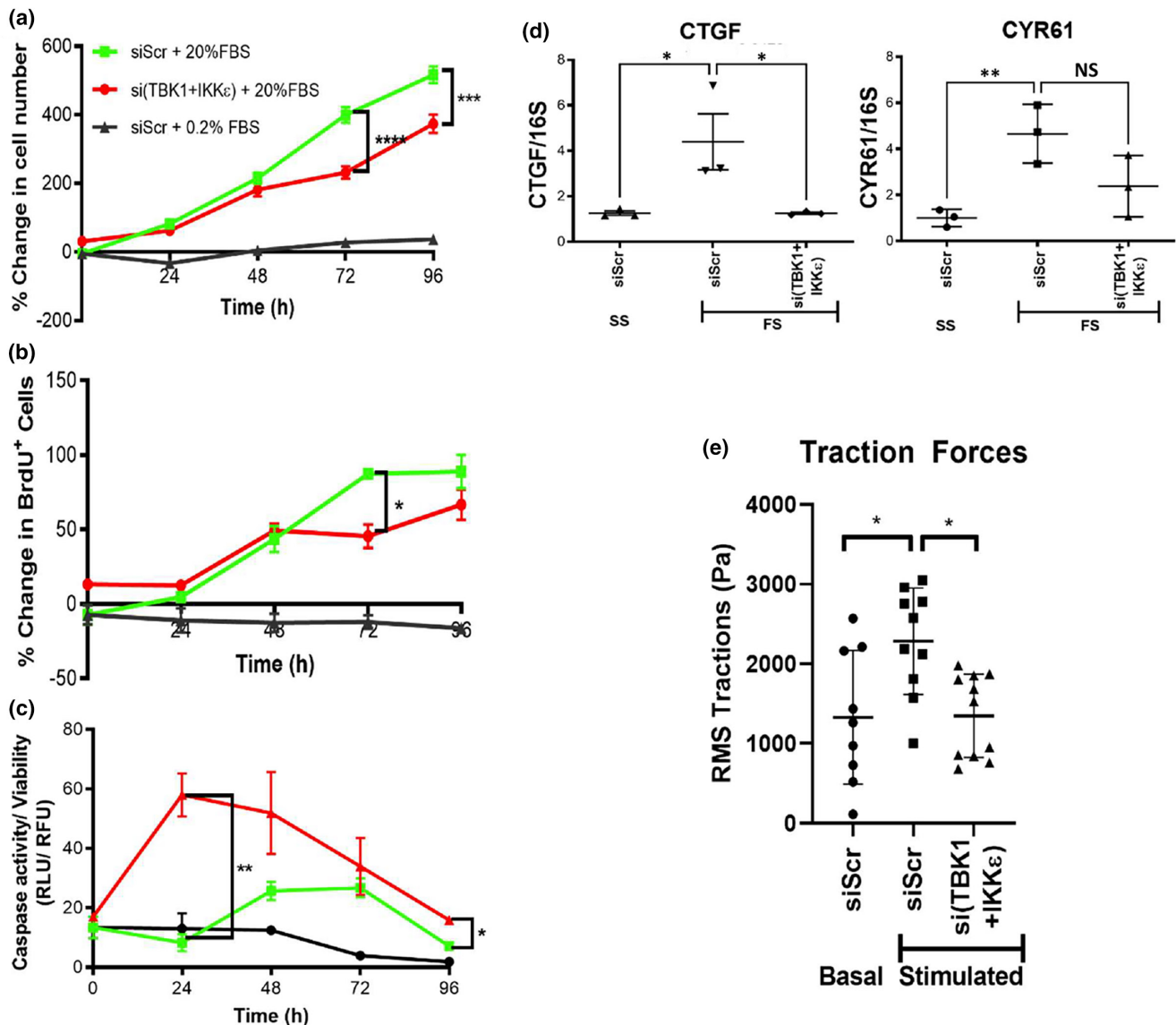


**FIGURE 4** TBK1/IKK $\epsilon$  knockdown reduces PASC proliferation and contractile capacity. PASC were grown in 20% FBS media transfected with siRNA scrambled control (si-Scr) or targeting both TBK1 and IKK $\epsilon$  (si-(TBK1+IKK $\epsilon$ )); as a comparison PASC were grown in 0.2% FBS plus si-Scr. Data in (a) and (b) are normalized to baseline controls collected at the time of siRNA treatment ~16h prior to FBS stimulation. The PASCs transfected with TBK1/IKK $\epsilon$  showed (a) a net reduction in cell number at 72h and 96h, (b) lower proliferation at 72h, and (c) increased apoptosis at 24h. PASCs transfected with si-TBK1/IKK $\epsilon$  also showed lower gene expression of (d) YAP/TAZ target genes CTGF and CYR61 in 20% FBS (FS), comparable to control levels seen in 0.2% FBS media (SS). (d) PASCs increased root mean square (RMS) tractions when stimulated with TGF- $\beta$  (6 ng/mL) and ET-1 (100 ng/mL) (Stimulated); this response was ablated by siRNA targeting TBK1 and IKK $\epsilon$ . Tukey post-test: Significance designated \* $p < 0.05$ , \*\* $p < 0.01$ , and \*\*\* $p < 0.001$ . Horizontal lines indicate mean values. Data represent three or more biological experiments.

incorporation) (Figure 4b), and apoptosis (by caspase activity/viability) (Figure 4c). Knockdown of TBK1/IKK $\epsilon$  significantly decreased proliferation (Figure 4b) and increased apoptosis (Figure 4c) with an overall reduction in PASC cell number compared with controls at 72 h (Figure 4a). Furthermore, knockdown of TBK1/IKK $\epsilon$  significantly reduced transcript levels of YAP/TAZ target genes *CTGF* and *CYR61* in 20% FBS-stimulated PASC compared with controls (Figure 4d), consistent with our observations of reduced YAP/TAZ protein and nuclear localization under these conditions. Knockdown of TBK1/IKK $\epsilon$  also significantly attenuated contractility, as assessed by traction microscopy, in TGF- $\beta$ /ET-1-stimulated PASCs (Figure 4e). These results demonstrate that a targeted specific reduction of non-canonical IKB kinase expression significantly diminishes multiple PAH-associated vascular remodeling behaviors in PASCs.

### 3.5 | TBK1/IKK $\epsilon$ chemical inhibitors reduce active YAP/TAZ, cell number, and YAP/TAZ target genes in PASC

To test the effect of chemical inhibitors of non-canonical IKB kinases on PAH-associated vascular remodeling behaviors in PASC, cells were stimulated with 20% FBS-containing media. Treprostinil was used as an approved PAH therapeutic known to modulate YAP/TAZ via prostacyclin receptor activation (Liu et al., 2016; Zmajkovicova et al., 2019). Amlexanox (a non-specific non-canonical IKB kinase inhibitor), Compound I and Compound II (new generation of non-canonical IKB kinase inhibitors) were administered over a concentration range of 0.03–30.0  $\mu$ M. To determine the short- and long-term effects of non-canonical IKB kinase inhibitors on YAP/TAZ activity, nuclear (active) YAP/TAZ levels were assessed at 2 and 10 h after treatment (Figure 5a). Treprostinil reduced

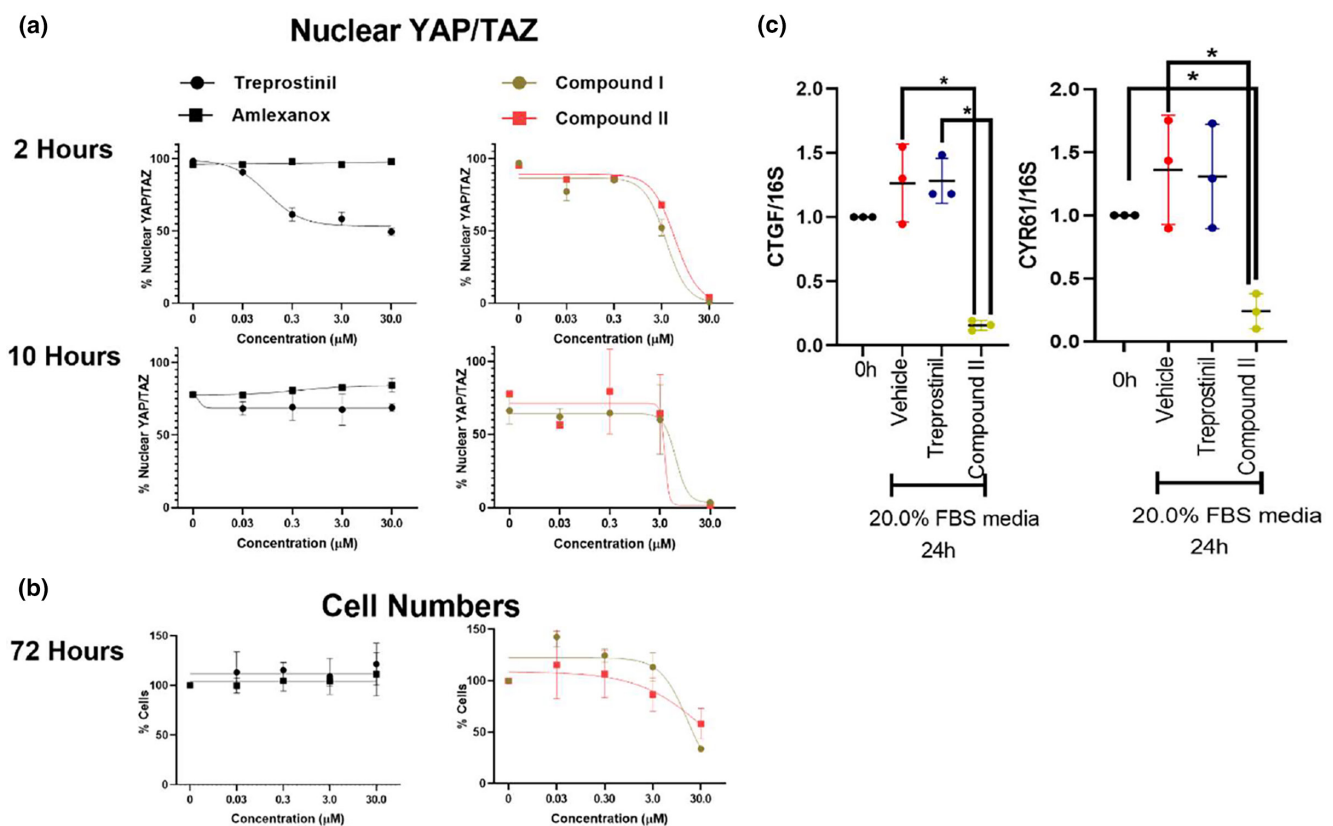


**FIGURE 5** TBK1/IKK $\epsilon$  inhibitors durably reduce nuclear YAP/TAZ, cell number, and YAP/TAZ target genes in PASC. PASC were stimulated with 20.0% FBS and treated with TBK1/IKK $\epsilon$  inhibitors (amlexanox, Compound I, or Compound II), or the prostacyclin analog treprostinil (Trp). (a) YAP/TAZ nuclear levels were stably reduced in a dose-dependent fashion at both 2 and 10 h after treatment with Compound I and Compound II. In contrast, amlexanox was ineffective, while treprostinil was potent but exerted only short-duration effect at 2 h that was absent at 10 h. (b) Consistent with durable effects of Compounds I and II, cell numbers were also dose-dependently reduced over 72 h of treatment, whereas no effect was seen with treprostinil. (c) Treatment of PASC with Compound II durably reduced YAP/TAZ target genes *CTGF* and *CYR61* levels 24 h after treatment, whereas treprostinil showed no effect at this time point. 5  $\mu$ M of treprostinil, Compound II, or equivalent volume of DMSO (vehicle) were used in the experiment. One-Way ANOVA and Tukey post-test: Significance designated \* $p$  < 0.05. Horizontal lines indicate mean values. Data represent three or more biological experiments.

nuclear YAP/TAZ expression in a dose-dependent manner at 2h but was ineffective at 10h. Amlexanox had no measurable effect, but both Compound I and Compound II showed dose-dependent decreases in active YAP/TAZ at 2h that were sustained out to 10h. These results suggest that effective inhibition of non-canonical IKB kinases can reduce YAP/TAZ activation for prolonged periods of time and may have more sustained effects on YAP/TAZ inactivation in PSMCs than treprostinil.

We also examined the impact of non-canonical IKB kinase inhibitors on PSMC cell number at 72h in 20% FBS-containing media (Figure 5b). Neither amlexanox nor treprostinil had any effect on PSMC cell number at this extended duration. However, both Compound I and Compound II reduced PSMC numbers at 48 and 72h, likely as one consequence of the prolonged YAP/TAZ inactivation observed with these non-canonical IKB kinase inhibitors. Compound II was subsequently selected to be examined in comparison with treprostinil for its ability to modulate expression of YAP/TAZ downstream target genes. After 24h of stimulation with 20% FBS-containing media, cells treated with Compound II showed significantly lower expression of YAP/TAZ target genes CTGF and CYR61 compared with vehicle control and treprostinil-treated PSMC groups (Figure 5c). These results highlight the potential of non-canonical IKB kinase inhibitors to have a prolonged effect on proliferation and YAP/TAZ activity in PSMCs compared with prostacyclin analogs such as treprostinil.

## 4 | DISCUSSION

The goal of this study was to determine if non-canonical IKB kinases could be targeted to attenuate PAH-associated pathological vascular remodeling behaviors and YAP/TAZ activation in PSMCs. Our previous work has demonstrated a key role for YAP/TAZ in driving vascular remodeling phenotypes in PSMCs (Dieffenbach et al., 2017). Our results show that TBK1/IKK $\epsilon$  are activated in a rat model of PH and that cytokines implicated in PAH can activate TBK1/IKK $\epsilon$  and YAP/TAZ in PSMCs. We also found that reducing the activity/levels of non-canonical IKB kinases TBK1/IKK $\epsilon$  decreased expression/activation of transcription factors YAP/TAZ in PSMCs. In addition to prolonged inactivation of YAP/TAZ, inhibition of TBK1/IKK $\epsilon$  reduced proliferation, enhanced apoptosis, and decreased contractility in PSMCs, indicative of attenuating PAH-associated vascular remodeling behaviors. These findings strongly suggest that the inhibition of non-canonical IKB kinases offers a novel route to modulate YAP/TAZ in PSMCs in PAH.

System analysis of the human pulmonary arterial hypertension lung transcriptome previously showed an activation

signature for several genes in the non-canonical IKB kinase pathway including TBK1/IKK $\epsilon$ , and interferon regulatory factors (IRF3/7) (Stearman et al., 2019). Several mediators and effectors of the non-canonical IKB kinase pathway such as interleukin 1 $\beta$  (IL1 $\beta$ ), Toll-like receptors (TLRs), and interferon  $\gamma$  (IFN $\gamma$ ) were seen upregulated in a meta-analysis of PAH blood genome (Elinoff et al., 2020). While most of our knowledge on non-canonical IKB kinases comes from studies of innate immunity and cancer, the role of these kinases in a host of other pathophysiological signaling such as inflammation, cancer, diabetes, obesity, neurological disorders, and pulmonary fibrosis is rapidly emerging. Several diverse signaling events occur upstream of non-canonical IKB kinase activation. Membrane-bound TLRs, pattern recognition receptors (PRRs), or the cytosolic RNA and DNA sensors can activate TBK1/IKK $\epsilon$ . Hence several cytokines, pathogen-associated molecular patterns (PAMPS), and damage-associated molecular patterns (DAMPs) can be upstream of these kinases and facilitate signaling in the non-canonical IKB kinase pathway.

Of potential relevance to TBK1/IKK $\epsilon$  activation in PAH, the initial oxidative stress/toxin-induced endothelial injury of the pulmonary vasculature can lead to production of DAMPs (Kato et al., 2017; Mendonça et al., 2016). In addition, vasoconstriction that ensues from vascular remodeling in the endothelium may activate the inflammatory NF-KB signaling pathway through TLR2 receptors (Li et al., 2013; Tan et al., 2014). A transcriptomic analysis of the MCT rat model of PH showed upregulation of DAMPs and an increase in TLR signaling (Xiao et al., 2020). PAMPS released by pathogens may also induce inflammation in PAH. Inflammation is a key characteristic feature of PAH and correlates with greater morbidity and mortality in PAH patients (Cracowski et al., 2014; Soon et al., 2010). Marked pulmonary perivascular inflammation correlates with intima and media remodeling in PAH and points to the role of inflammation in PAH-associated vascular remodeling (Stacher et al., 2012). In animal models of PH (both MCT and Sugen/Hypoxia models), an inflammatory vascular response precedes the development of experimental PH (Meloche et al., 2017; Nogueira-Ferreira et al., 2015). Furthermore, TNF- $\alpha$  and IL-1 $\beta$  are known to decrease prostacyclin synthesis and worsen disease in rat models of PH (Itoh et al., 2003). While the importance of inflammation in PAH is well established (Rabinovitch et al., 2014), the exact mechanism of inflammatory signaling in PAH pathogenesis remains unclear (Stacher et al., 2012). Our results support a novel potential link between inflammatory pathways and YAP/TAZ-mediated PAH remodeling phenotypes via the non-canonical IKB kinase pathway.

Several studies have also shown that YAP/TAZ may be activated in PAH via the altered mechanobiological

environment of the remodeled vessels (Bertero et al., 2016; Dieffenbach et al., 2017; Liu et al., 2016). Moreover, reducing YAP/TAZ activation in the pulmonary vasculature ameliorates PH (Bertero et al., 2016; Zuo et al., 2021) in animal models. However, YAP/TAZ play critical roles in several cellular processes such as proliferation, differentiation, mechanoregulation, and development (Pocaterra et al., 2020). Hence, complete inhibition of YAP/TAZ in all cell types may be deleterious, even though drugs such as verteporfin and ROCK inhibitors could achieve that (Brouwer et al., 2021; Gibault et al., 2017; Noguchi et al., 2018). Understanding and targeting signaling events upstream of YAP/TAZ provides an opportunity to confine and target the effects of YAP/TAZ modulation to specific cell types/compartments of the cell avoiding deleterious side effects and maximizing efficacy in diseases driven by activation of YAP/TAZ, such as PAH. We show here that inhibition of non-canonical IKB kinase pathway inhibits YAP/TAZ signaling downstream of multiple stimuli in PSMCs, highlighting its potential value.

Our prior work had shown the ability of non-canonical IKB kinase TBK1 to regulate YAP/TAZ and the fibrogenic phenotype in pulmonary fibroblasts (Aravamudhan et al., 2020). IPF and IPAH share several common features and biological pathways. In a study comparing the pulmonary vascular gene expression profiles of patients with IPF and those who had consequent PH, no remarkable difference was found indicating that the pulmonary arteriolar changes in IPF and PH could have similar underlying mechanisms (Patel et al., 2013). However, another study comparing the lung gene expression profiles of patients with pulmonary fibrosis (PF) but no PH versus patients who had PF associated PH (APH) showed differential pathway regulation with the PF group being defined by a pro-inflammatory signature and the APH group being more pro-proliferative (Mura et al., 2012). Here, we showed that the link between non-canonical IKB kinases and YAP/TAZ we observed in pulmonary fibroblasts extends to PSMCs, the matrix producing, contractile cells of the pulmonary vasculature implicated in PAH-associated remodeling. Our results showed that TBK1/IKK $\epsilon$  activity is essential to maintain the levels of active YAP/TAZ in PSMCs. Reducing TBK1/IKK $\epsilon$  activity decreased active YAP/TAZ and attenuated PAH-associated remodeling phenotypes for a sustained period compared with treprostinil, a currently approved PAH treatment, which was short-acting. This finding points to a potential advantage in the durability of response in targeting PSMC YAP/TAZ activation via inhibition of non-canonical IKB kinase pathway rather than agonism of the prostacyclin receptor.

Our study has several limitations. While our human cell studies confirmed TBK1/IKK $\epsilon$  relevance in human cells from males and females, we analyzed *in vivo* TBK1/

IKK $\epsilon$  activation in only male rats, and future work should extend these observations to females. We used a limited number of primary human PSMCs and observed substantial donor-to-donor biological variability in some TBK1/IKK $\epsilon$  responses. PAH is a heterogeneous disease and testing in larger populations of human cells will be needed to assess the broader utility of TBK1/IKK $\epsilon$  inhibition in targeting PAH-associated vascular remodeling behaviors. Similarly, testing of TBK1/IKK $\epsilon$  inhibitors in pre-clinical animal models of PAH will be needed to evaluate their safety and potential efficacy for PAH treatment.

In conclusion, our results demonstrate that reducing the activity or expression of TBK1/IKK $\epsilon$  in PSMCs attenuates YAP/TAZ activation and vascular remodeling phenotypes. TBK1/IKK $\epsilon$  are activated by inflammatory PAH-associated cytokines and serve an essential role in YAP/TAZ protein stability by affecting YAP phosphorylation. Thus, we have identified non-canonical IKB kinases TBK1/IKK $\epsilon$  as important regulators linking cytokine-based activation of YAP/TAZ in PSMCs. A new generation of TBK1/IKK $\epsilon$  inhibitors with greater specificity and less toxicity are being discovered (Niederberger et al., 2013), providing a multitude of options to target the pathway. These results indicate that TBK1/IKK $\epsilon$  inhibitors may offer a novel therapeutic approach to reduce YAP/TAZ activation and attenuate PSMC activation and downstream vascular remodeling in PAH.

## ACKNOWLEDGMENTS

We thank Dr. Kate Fitzgerald from the UMass Chan Medical School for providing pcDNA3-Flag-TBK1 and pcDNA3-Flag-TBK1(K38A) plasmids.

## FUNDING INFORMATION

This work was supported by National Heart, Lung, and Blood Institute Grants 5R01HL137366-04 (to L.E.F. and D.J.T.); K08 HL-143197 (to P.B.D.); American Heart Association (AHA) Grant-in-Aid 17GRNT33660449 (to L.E.F.) and AHA Grant 20POST35210650 (to A.A.), HL105355 (to P.A.L.), HL158018 (to P.A.L.), and HL153026 (to P.A.L.).

## CONFLICT OF INTEREST STATEMENT


No conflicts of interest, financial or otherwise, are declared by the authors.

## ETHICS STATEMENT

All animal experiments were performed in compliance with the laws and guidelines as set forth by the Harvard Medical area standing committee on animals and the Lovelace Respiratory Research Institute Animal Care and Use Committee. Human tissue samples and cell lines were obtained from Pulmonary Hypertension Breakthrough

Initiative (PHBI) and under protocol approved by the Partners Research Committee. Informed consent was obtained by the PHBI from the subjects or their legal guardian prior to enrolling in the study.

## ORCID

Daniel J. Tschumperlin  <https://orcid.org/0000-0002-5115-9025>

## REFERENCES

- Aldred, M. A., Vijaykrishnan, J., James, V., Soubrier, F., Gomez-Sanchez, M. A., Martensson, G., Galie, N., Manes, A., Corris, P., & Simonneau, G. (2006). BMP2 gene rearrangements account for a significant proportion of mutations in familial and idiopathic pulmonary arterial hypertension. *Human Mutation*, *27*, 212–213.
- Andruska, A., & Spiekerkoetter, E. (2018). Consequences of BMP2 deficiency in the pulmonary vasculature and beyond: Contributions to pulmonary arterial hypertension. *International Journal of Molecular Sciences*, *19*, 2499.
- Aravamudhan, A., Haak, A. J., Choi, K. M., Meridew, J. A., Caporarello, N., Jones, D. L., Tan, Q., Ligresti, G., & Tschumperlin, D. J. (2020). TBK1 regulates YAP/TAZ and fibrogenic fibroblast activation. *American Journal of Physiology. Lung Cellular and Molecular Physiology*, *318*, L852–L863.
- Aravamudhan, A., Ramos, D. M., Nip, J., Kalajzic, I., & Kumbar, S. G. (2018). Micro-nanostructures of cellulose-collagen for critical sized bone defect healing. *Macromolecular Bioscience*, *18*, 1700263.
- Bertero, T., Cottrill, K. A., Lu, Y., Haeger, C. M., Dieffenbach, P., Annis, S., Hale, A., Bhat, B., Kaimal, V., & Zhang, Y.-Y. (2015). Matrix remodeling promotes pulmonary hypertension through feedback mechanoactivation of the YAP/TAZ-miR-130/301 circuit. *Cell Reports*, *13*, 1016–1032.
- Bertero, T., Oldham, W. M., Cottrill, K. A., Pisano, S., Vanderpool, R. R., Yu, Q., Zhao, J., Tai, Y., Tang, Y., Zhang, Y. Y., Rehman, S., Sugahara, M., Qi, Z., Gorcsan, J., 3rd, Vargas, S. O., Saggari, R., Saggari, R., Wallace, W. D., Ross, D. J., ... Chan, S. Y. (2016). Vascular stiffness mechanoactivates YAP/TAZ-dependent glutaminolysis to drive pulmonary hypertension. *The Journal of Clinical Investigation*, *126*, 3313–3335.
- Brasier, A. R. (2010). The nuclear factor- $\kappa$ B-interleukin-6 signalling pathway mediating vascular inflammation. *Cardiovascular Research*, *86*, 211–218.
- Brouwer, N. J., Konstantinou, E. K., Gragoudas, E. S., Marinkovic, M., Luyten, G. P., Kim, I. K., Jager, M. J., & Vavvas, D. G. (2021). Targeting the YAP/TAZ pathway in uveal and conjunctival melanoma with verteporfin. *Investigative Ophthalmology & Visual Science*, *62*, 3.
- Cogan, J. D., Pauciulo, M. W., Batchman, A. P., Prince, M. A., Robbins, I. M., Hedges, L. K., Stanton, K. C., Wheeler, L. A., Phillips, J. A., III, & Loyd, J. E. (2006). High frequency of BMP2 exonic deletions/duplications in familial pulmonary arterial hypertension. *American Journal of Respiratory and Critical Care Medicine*, *174*, 590–598.
- Cracowski, J.-L., Chabot, F., Labarère, J., Faure, P., Degano, B., Schwebel, C., Chaouat, A., Reynaud-Gaubert, M., Cracowski, C., & Sitbon, O. (2014). Proinflammatory cytokine levels are linked to death in pulmonary arterial hypertension. *European Respiratory Journal*, *43*, 915–917.
- Dieffenbach, P. B., Haeger, C. M., Coronata, A. M. F., Choi, K. M., Varelas, X., Tschumperlin, D. J., & Fredenburgh, L. E. (2017). Arterial stiffness induces remodeling phenotypes in pulmonary artery smooth muscle cells via YAP/TAZ-mediated repression of cyclooxygenase-2. *American Journal of Physiology. Lung Cellular and Molecular Physiology*, *313*, L628–L647.
- Dorfmueller, P., Perros, F., Balabanian, K., & Humbert, M. (2003). Inflammation in pulmonary arterial hypertension. *European Respiratory Journal*, *22*, 358–363.
- Elinoff, J. M., Mazer, A. J., Cai, R., Lu, M., Graninger, G., Harper, B., Ferreyra, G. A., Sun, J., Solomon, M. A., & Danner, R. L. (2020). Meta-analysis of blood genome-wide expression profiling studies in pulmonary arterial hypertension. *American Journal of Physiology. Lung Cellular and Molecular Physiology*, *318*, L98–L111.
- Fares, W. H. (2015). Orenitram... not verified. *American Journal of Respiratory and Critical Care Medicine*, *191*, 713–714.
- Fitzgerald, K. A., McWhirter, S. M., Faia, K. L., Rowe, D. C., Latz, E., Golenbock, D. T., Coyle, A. J., Liao, S.-M., & Maniatis, T. (2003). IKK $\epsilon$  and TBK1 are essential components of the IRF3 signaling pathway. *Nature Immunology*, *4*, 491–496.
- Fujita, M., Shannon, J. M., Irvin, C. G., Fagan, K. A., Cool, C., Augustin, A., & Mason, R. J. (2001). Overexpression of tumor necrosis factor- $\alpha$  produces an increase in lung volumes and pulmonary hypertension. *American Journal of Physiology. Lung Cellular and Molecular Physiology*, *280*, L39–L49.
- Galie, N., Hoeper, M. M., Humbert, M., Torbicki, A., Vachiery, J.-L., Barbera, J. A., Beghetti, M., Corris, P., Gaine, S., & Gibbs, J. S. (2009). Guidelines for the diagnosis and treatment of pulmonary hypertension: The task force for the diagnosis and treatment of pulmonary hypertension of the European Society of Cardiology (ESC) and the European Respiratory Society (ERS), endorsed by the International Society of Heart and Lung Transplantation (ISHLT). *European Heart Journal*, *30*, 2493–2537.
- Garcia, G., Jr., Paul, S., Beshara, S., Ramanujan, V. K., Ramaiah, A., Nielsen-Saines, K., Li, M. M. H., French, S. W., Morizono, K., Kumar, A., & Arumugaswami, V. (2020). Hippo signaling pathway has a critical role in Zika virus replication and in the pathogenesis of Neuroinflammation. *The American Journal of Pathology*, *190*, 844–861.
- Gibault, F., Bailly, F., Corvaisier, M., Coevoet, M., Huet, G., Melnyk, P., & Cotellet, P. (2017). Molecular features of the YAP inhibitor verteporfin: Synthesis of hexasubstituted dipyrroles as potential inhibitors of YAP/TAZ, the downstream effectors of the hippo pathway. *ChemMedChem*, *12*, 954–961.
- Haak, A. J., Kostallari, E., Sicard, D., Ligresti, G., Choi, K. M., Caporarello, N., Jones, D. L., Tan, Q., Meridew, J., & Diaz Espinosa, A. M. (2019). Selective YAP/TAZ inhibition in fibroblasts via dopamine receptor D1 agonism reverses fibrosis. *Science Translational Medicine*, *11*, eaau6296.
- Hagen, M., Fagan, K., Steudel, W., Carr, M., Lane, K., Rodman, D. M., & West, J. (2007). Interaction of interleukin-6 and the BMP pathway in pulmonary smooth muscle. *American Journal of Physiology. Lung Cellular and Molecular Physiology*, *292*, L1473–L1479.
- Hiepen, C., Jatzlau, J., Hildebrandt, S., Kampfrath, B., Goktas, M., Murgai, A., Cuellar Camacho, J. L., Haag, R., Ruppert, C., &

- Sengle, G. (2019). BMPR2 acts as a gatekeeper to protect endothelial cells from increased TGF $\beta$  responses and altered cell mechanics. *PLoS Biology*, *17*, e3000557.
- Itoh, A., Nishihira, J., Makita, H., Miyamoto, K., Yamaguchi, E., & Nishimura, M. (2003). Effects of IL-1 $\beta$ , TNF- $\alpha$ , and macrophage migration inhibitory factor on prostacyclin synthesis in rat pulmonary artery smooth muscle cells. *Respirology*, *8*, 467–472.
- Kato, G. J., Steinberg, M. H., & Gladwin, M. T. (2017). Intravascular hemolysis and the pathophysiology of sickle cell disease. *The Journal of Clinical Investigation*, *127*, 750–760.
- Landt, S. G., Marinov, G. K., Kundaje, A., Kheradpour, P., Pauli, F., Batzoglou, S., Bernstein, B. E., Bickel, P., Brown, J. B., Cayting, P., Chen, Y., DeSalvo, G., Epstein, C., Fisher-Aylor, K. I., Euskirchen, G., Gerstein, M., Gertz, J., Hartemink, A. J., Hoffman, M. M., ... Snyder, M. (2012). ChIP-seq guidelines and practices of the ENCODE and modENCODE consortia. *Genome Research*, *22*, 1813–1831.
- Li, M., Tan, Y., Stenmark, K. R., & Tan, W. (2013). High pulsatility flow induces acute endothelial inflammation through overpolarizing cells to activate NF- $\kappa$ B. *Cardiovascular Engineering and Technology*, *4*, 26–38.
- Liu, F., Haeger, C. M., Dieffenbach, P. B., Sicard, D., Chrobak, I., Coronata, A. M. F., Velandia, M. M. S., Vitali, S., Colas, R. A., & Norris, P. C. (2016). Distal vessel stiffening is an early and pivotal mechanobiological regulator of vascular remodeling and pulmonary hypertension. *JCI Insight*, *1*, e86987.
- Malenfant, S., Neyron, A.-S., Paulin, R., Potus, F., Meloche, J., Provencher, S., & Bonnet, S. (2013). Signal transduction in the development of pulmonary arterial hypertension. *Pulmonary Circulation*, *3*, 278–293.
- Marinković, A., Mih, J. D., Park, J. A., Liu, F., & Tschumperlin, D. J. (2012). Improved throughput traction microscopy reveals pivotal role for matrix stiffness in fibroblast contractility and TGF- $\beta$  responsiveness. *American Journal of Physiology. Lung Cellular and Molecular Physiology*, *303*, L169–L180.
- Meloche, J., Lampron, M.-C., Nadeau, V., Maltais, M., Potus, F., Lambert, C., Tremblay, E., Vitry, G., Breuils-Bonnet, S., & Boucherat, O. (2017). Implication of inflammation and epigenetic readers in coronary artery remodeling in patients with pulmonary arterial hypertension. *Arteriosclerosis, Thrombosis, and Vascular Biology*, *37*, 1513–1523.
- Mendonça, R., Silveira, A. A., & Conran, N. (2016). Red cell DAMPs and inflammation. *Inflammation Research*, *65*, 665–678.
- Mura, M., Anraku, M., Yun, Z., McRae, K., Liu, M., Waddell, T. K., Singer, L. G., Granton, J. T., Keshavjee, S., & de Perrot, M. (2012). Gene expression profiling in the lungs of patients with pulmonary hypertension associated with pulmonary fibrosis. *Chest*, *141*, 661–673.
- Newman, J. H., Trembath, R. C., Morse, J. A., Grunig, E., Loyd, J. E., Adnot, S., Coccio, F., Ventura, C., Phillips, J. A., & Knowles, J. A. (2004). Genetic basis of pulmonary arterial hypertension: Current understanding and future directions. *Journal of the American College of Cardiology*, *43*, S33–S39.
- Niederberger, E., V Moser, C., L Kynast, K., & Geisslinger, G. (2013). The non-canonical I $\kappa$ B kinases IKK $\epsilon$  and TBK1 as potential targets for the development of novel therapeutic drugs. *Current Molecular Medicine*, *13*, 1089–1097.
- Noguchi, S., Saito, A., & Nagase, T. (2018). YAP/TAZ signaling as a molecular link between fibrosis and cancer. *International Journal of Molecular Sciences*, *19*, 3674.
- Nogueira-Ferreira, R., Vitorino, R., Ferreira, R., & Henriques-Coelho, T. (2015). Exploring the monocrotaline animal model for the study of pulmonary arterial hypertension: A network approach. *Pulmonary Pharmacology & Therapeutics*, *35*, 8–16.
- Patel, N. M., Kawut, S. M., Jelic, S., Arcasoy, S. M., Lederer, D. J., & Borczuk, A. C. (2013). Pulmonary arteriole gene expression signature in idiopathic pulmonary fibrosis. *European Respiratory Journal*, *41*, 1324–1330.
- Patel, S. J., King, K. R., Casali, M., & Yarmush, M. L. (2009). DNA-triggered innate immune responses are propagated by gap junction communication. *Proceedings of the National Academy of Sciences*, *106*, 12867–12872.
- Peters, R. T., Liao, S.-M., & Maniatis, T. (2000). IKK $\epsilon$  is part of a novel PMA-inducible I $\kappa$ B kinase complex. *Molecular Cell*, *5*, 513–522.
- Pocaterra, A., Romani, P., & Dupont, S. (2020). YAP/TAZ functions and their regulation at a glance. *Journal of Cell Science*, *133*, jcs230425.
- Pomerantz, J. L., & Baltimore, D. (1999). NF- $\kappa$ B activation by a signaling complex containing TRAF2, TANK and TBK1, a novel IKK-related kinase. *The EMBO Journal*, *18*, 6694–6704.
- Pullamsetti, S. S., Savai, R., Seeger, W., & Goncharova, E. A. (2017). Translational advances in the field of pulmonary hypertension. From cancer biology to new pulmonary arterial hypertension therapeutics. Targeting cell growth and proliferation signaling hubs. *American Journal of Respiratory and Critical Care Medicine*, *195*, 425–437.
- Rabinovitch, M., Guignabert, C., Humbert, M., & Nicolls, M. R. (2014). Inflammation and immunity in the pathogenesis of pulmonary arterial hypertension. *Circulation Research*, *115*, 165–175.
- Rohm, I., Grün, K., Müller, L. M., Bäß, L., Förster, M., Schreppe, A., Kretschmar, D., Pistulli, R., Yilmaz, A., & Bauer, R. (2019). Cellular inflammation in pulmonary hypertension: Detailed analysis of lung and right ventricular tissue, circulating immune cells and effects of a dual endothelin receptor antagonist. *Clinical Hemorheology and Microcirculation*, *73*, 497–522.
- Ruffenach, G., Umar, S., Vaillancourt, M., Hong, J., Cao, N., Sarji, S., Moazeni, S., Cunningham, C. M., Ardehali, A., & Reddy, S. T. (2019). Histological hallmarks and role of slug/PIP axis in pulmonary hypertension secondary to pulmonary fibrosis. *EMBO Molecular Medicine*, *11*, e10061.
- Sanjabi, S., Williams, K. J., Sacconi, S., Zhou, L., Hoffmann, A., Ghosh, G., Gerondakis, S., Natoli, G., & Smale, S. T. (2005). A c-Rel subdomain responsible for enhanced DNA-binding affinity and selective gene activation. *Genes & Development*, *19*, 2138–2151.
- Shimada, T., Kawai, T., Takeda, K., Matsumoto, M., Inoue, J., Tatsumi, Y., Kanamaru, A., & Akira, S. (1999). IKK-i, a novel lipopolysaccharide-inducible kinase that is related to IkappaB kinases. *International Immunology*, *11*, 1357–1362.
- Sitbon, O., & Noordegraaf, A. V. (2017). Epoprostenol and pulmonary arterial hypertension: 20 years of clinical experience. *European Respiratory Review*, *26*, 160055.
- Soon, E., Holmes, A. M., Treacy, C. M., Doughty, N. J., Southgate, L., Machado, R. D., Trembath, R. C., Jennings, S., Barker, L., Nicklin, P., Walker, C., Budd, D. C., Pepke-Zaba, J., & Morrell, N. W. (2010). Elevated levels of inflammatory cytokines predict survival in idiopathic and familial pulmonary arterial hypertension. *Circulation*, *122*, 920–927.

- Stacher, E., Graham, B. B., Hunt, J. M., Gandjeva, A., Groshong, S. D., McLaughlin, V. V., Jessup, M., Grizzle, W. E., Aldred, M. A., & Cool, C. D. (2012). Modern age pathology of pulmonary arterial hypertension. *American Journal of Respiratory and Critical Care Medicine*, *186*, 261–272.
- Stearman, R. S., Bui, Q. M., Speyer, G., Handen, A., Cornelius, A. R., Graham, B. B., Kim, S., Mickler, E. A., Tuder, R. M., & Chan, S. Y. (2019). Systems analysis of the human pulmonary arterial hypertension lung transcriptome. *American Journal of Respiratory Cell and Molecular Biology*, *60*, 637–649.
- Steiner, M. K., Syrkina, O. L., Kolliputi, N., Mark, E. J., Hales, C. A., & Waxman, A. B. (2009). Interleukin-6 overexpression induces pulmonary hypertension. *Circulation Research*, *104*, 236–244.
- Stevens, T., Janssen, P. L., & Tucker, A. (1992). Acute and long-term TNF- $\alpha$  administration increases pulmonary vascular reactivity in isolated rat lungs. *Journal of Applied Physiology*, *73*, 708–712.
- Tan, Y., Tseng, P.-O., Wang, D., Zhang, H., Hunter, K., Hertzberg, J., Stenmark, K. R., & Tan, W. (2014). Stiffening-induced high pulsatility flow activates endothelial inflammation via a TLR2/NF- $\kappa$ B pathway. *PLoS One*, *9*, e102195.
- Voelkel, N. F., Tuder, R. M., Bridges, J., & Arend, W. P. (1994). Interleukin-1 receptor antagonist treatment reduces pulmonary hypertension generated in rats by monocrotaline. *American Journal of Respiratory Cell and Molecular Biology*, *11*, 664–675.
- Wang, Q., Zuo, X. R., Wang, Y. Y., Xie, W. P., Wang, H., & Zhang, M. (2013). Monocrotaline-induced pulmonary arterial hypertension is attenuated by TNF- $\alpha$  antagonists via the suppression of TNF- $\alpha$  expression and NF- $\kappa$ B pathway in rats. *Vascular Pharmacology*, *58*, 71–77.
- Xiao, G., Zhuang, W., Wang, T., Lian, G., Luo, L., Ye, C., Wang, H., & Xie, L. (2020). Transcriptomic analysis identifies toll-like and nod-like pathways and necroptosis in pulmonary arterial hypertension. *Journal of Cellular and Molecular Medicine*, *24*, 11409–11421.
- Xie, H., Wu, L., Deng, Z., Huo, Y., & Cheng, Y. (2018). Emerging roles of YAP/TAZ in lung physiology and diseases. *Life Sciences*, *214*, 176–183.
- Yu, T., Yi, Y.-S., Yang, Y., Oh, J., Jeong, D., & Cho, J. Y. (2012). The pivotal role of TBK1 in inflammatory responses mediated by macrophages. *Mediators of Inflammation*, *2012*, 1–8.
- Zhang, Q., Meng, F., Chen, S., Plouffe, S. W., Wu, S., Liu, S., Li, X., Zhou, R., Wang, J., Zhao, B., Liu, J., Qin, J., Zou, J., Feng, X. H., Guan, K. L., & Xu, P. (2017). Hippo signalling governs cytosolic nucleic acid sensing through YAP/TAZ-mediated TBK1 blockade. *Nature Cell Biology*, *19*, 362–374.
- Zmajkovicova, K., Menyhart, K., Bauer, Y., Studer, R., Renault, B., Schnoebelen, M., Bolinger, M., Nayler, O., & Gatfield, J. (2019). The antifibrotic activity of prostacyclin receptor agonism is mediated through inhibition of YAP/TAZ. *American Journal of Respiratory Cell and Molecular Biology*, *60*, 578–591.
- Zuo, W., Liu, N., Zeng, Y., Xiao, Z., Wu, K., Yang, F., Li, B., Song, Q., Xiao, Y., & Liu, Q. (2021). Luteolin ameliorates experimental pulmonary arterial hypertension via suppressing hippo-YAP/PI3K/AKT signaling pathway. *Frontiers in Pharmacology*, *12*, 663551.

**How to cite this article:** Aravamudhan, A., Dieffenbach, P. B., Choi, K. M., Link, P. A., Meridew, J. A., Haak, A. J., Fredenburgh, L. E., & Tschumperlin, D. J. (2024). Non-canonical IKB kinases regulate YAP/TAZ and pathological vascular remodeling behaviors in pulmonary artery smooth muscle cells. *Physiological Reports*, *12*, e15999. <https://doi.org/10.14814/phy2.15999>